Analytic modeling and risk assessment of aerial transmission of SARS-CoV-2 virus through vaping expirations in shared micro-environments

Roberto Sussman
Universidad Nacional Autonoma de Mexico https://orcid.org/0000-0003-3774-4452
Eliana Golberstein
Myriad Pharmaceutics
Riccardo Polosa (polosa@unict.it)
University of Catania https://orcid.org/0000-0002-8450-5721

Research

Keywords: SARS-CoV-2 COVID-19, electronic cigarettes, aerosol visibilty, risk modeling

Posted Date: March 31st, 2021

DOI: https://doi.org/10.21203/rs.3.rs-340115/v1

Analytic modeling and risk assessment of aerial transmission of SARS-CoV-2 virus through vaping expirations in shared micro-environments

Roberto A Sussman[a], Eliana Golberstein[b], Riccardo Polosa[1]

[a]*Instituto de Ciencias Nucleares, Universidad Nacional Autónoma de México, Ciudad de México, 04510, México*
[b]*Myriad Pharmaceuticals Limited, Unit 3, 36 Greenpark Rd, Penrose, 1061, Auckland, New Zealand*
[c]*Center of Excellence for the acceleration of HArm Reduction (CoEHAR) University of Catania, Italy*

Abstract

Background. E-cigarettes are an important harm reduction tool that provides smokers an alternative for nicotine consumption that is much safer than smoking. It is important to asses its safety under preventive and containment measures undertaken during the COVID-19 pandemic.

Methods. We develop a theoretical risk model to assess the contagion risk by aerial transmission of the SARS-CoV-2 virus carried by e–cigarette aerosol (ECA) in shared indoor spaces, a home and restaurant scenarios, with natural and mechanical ventilation, with and without face masks. We also provide the theoretical elements to explain the visibility of exhaled ECA, which has important safety implications.

Results. In a home or restaurant scenarios bystanders exposed to ECA expirations by an infectious vaper (and not wearing face masks) face a 1 % increase of risk of contagion with respect to a "control case" scenario defined by exclusively rest breathing without vaping. This relative added risk becomes $5-17$ % for high intensity vaping, $44-176$ % and over 260 % for speaking for various periods or coughing (all without vaping). Mechanical ventilation significantly decrease infective emissions but keep the same proportionality in risk percentages. Face masks of common usage effectively protect wearers from respiratory droplets and droplet nuclei possibly emitted by mask-less vapers as long as they avoid direct exposure to the visible exhaled vaping jet.

Conclusions. Vaping emissions in shared indoor spaces involve only a minuscule added risk of COVID-19 contagion with respect to the already existing (unavoidable) risk from continuous breathing, significantly less than speaking or coughing. Protection of bystanders from this contagion does not require extra preventive measures besides those already recommended (1.5 meters separation and wearing face masks).

Keywords: SARS-CoV-2 COVID-19, electronic cigarettes, aerosol visibilty, risk modeling

1. Introduction

As alternative products whose usage represents a minor fraction of health hazards associated with tobacco cigarettes, e-cigarettes have become a recognized harm reduction tool for millions

*Corresponding author
Email address: polosa@unict.it (Riccardo Polosa)

of smokers worldwide who are unable or unwilling to quit smoking by other means, Vapers, as users of these devices are known, are in various degrees living subjects of a personal decision to follow a tobacco harm reduction strategy that empowers them as consumers who desire to quit smoking to improve their health and welfare. This initiative contributes and complements the effort to address the global burden of harm caused by smoking. However, as all lifestyle and consumer habits in all walks of life, the personal harm reduction approach embodied in switching from smoking to vaping has been disrupted by preventive and containment measures implemented by health authorities worldwide to address the current COVID-19 pandemic, including various degrees of curtailment of social activities and home confinement recommendations and ordinances that have induced and/or required millions of vapers to share indoor spaces with non-vapers around them.

It is important to stress that vapers under confinement already perceive an important benefit that reinforces their harm reduction initiative: bystanders under confinement exposed to aerosol emissions from their e-cigarettes face only a negligible fraction of the hazard they would be facing if exposed to environmental tobacco smoke (as would be the case if home confined vapers had kept smoking). However, there is another worrying concern that can be very disruptive for vapers under these conditions, namely: the possibility that the environmental emissions of e-cigarette aerosol (ECA) that they exhale (if infected by the SARS-CoV-2 virus) could transmit COVID-19 to those sharing with them indoor spaces under home confinement or in other common spaces.

While there is evidence of contagion through respiratory droplet emissions from the usual respiratory activities, such as breathing vocalizing, coughing and sneezing, there is no data and/or direct evidence on this transmission through exhaled ECA. However, such possible COVID-19 contagion cannot be ruled our because vaping (like smoking) is a respiratory activity. Thus, a theoretically objective assessment of the risks involved in this possible contagion route is crucially necessary for the ongoing sustainment of the harm reduction approach pursued by millions of vapers under the prevailing conditions of the current pandemic. The present article addresses this necessity by providing a self-consistent risk model of COVID-19 contagion from this respiratory route in shared indoor spaces, considering relevant factors such as visibility, ventilation and face mask wearing.

Given the lack of empiric evidence of occurrence of COVID-19 contagion through exhaled ECA, and as a first approach, we have examined the plausibility and scope of droplet transmission through vaping expirations, taking cigarette smoking and mouth breathing as useful proxies for the respiratory mechanics and droplet emission that should occur through exhaled ECA modeled as an intermittent turbulent jet evolving into a puff (see Sussman et al. (2020)). We have also published a short paper Sussman et al. (2021) advancing some of the results of the present article, adding comment on related issues, such as the difference between exposure to exhaled ECA and environmental tobacco smoke, as well as a guideline for addressing these issues in public policies during the current pandemic.

In the present paper we consider the results of Sussman et al. (2020) to elaborate a risk evaluation of this transmission in shared indoor spaces: a home and restaurant scenarios with natural and mechanical ventilation, assuming that respiratory droplets have been uniformly distributed throughout the full indoor volume (hence bypassing the distinction between "droplets" and "aerosols"). Fort this purpose, we incorporate vaping exhalations into a simplified and modified version of the exponential dose-response reaction model developed by Buonanno et al. (2020a,b) (hereafter BMS), based on the notion of "*infective quanta*" (the virus concentration needed to infect 63 % of exposed individuals) constructed with actual data on SARS-CoV-2 infective parameters and considering the specifics of natural and mechanical ventilation. In order

to provide a more meaningful context, our risk model incorporates into the risk model results from Sussman et al. (2020) and BMS to evaluate viral quanta emissions, not only from vaping, but also from speaking and coughing, all compared with respect to a control state of unavoidable emissions from continuous breathing. We also discuss the risk involved for bystanders wearing face masks exposed to emissions from potentially infected unmasked individuals, as vapers must (at least) momentarily remove their face masks in order to vape.

We also discuss the visibility of exhaled ECA, which emerges from the optical properties of ECA droplets (light scattering Ruzer and Harley (2012)). This property has significant psychological and safety implications, namely: the fact that those surrounding potentially infectious vapers can instinctively place themselves away from the area of direct exposure clearly delineated by the visible exhaled cloud (something impossible to do with expirations from other respiratory activities, except smoking).

It is necessary to issue the following important disclaimer: the present article is concerned only with the risks of SARS-CoV-2 transmission through exhaled ECA, not with risks of COVID-19 infection or illness of vapers due to possible effects of vaping in the respiratory system, or other possible health hazards by users' exposure to inhaled ECA or bystanders to exhaled ECA derived from the usage of e-cigarettes as substitute of tobacco smoking. Readers are advised to consult the available literature on these subjects (see extensive reviews Farsalinos and Polosa (2014); RCP (2016); McNeill et al. (2018); NASEM (2018); Polosa et al. (2019)).

Another important disclaimer: we will not address risk of COVID-19 contagion through respiratory droplets carried by environmental tobacco smoke (ETS), though our risk evaluation on low intensity ('mouth to lung' puffing style practiced by 80-90 % of vapers) applies with some nuances to mainstream emissions of ETS (emerging from the smoker, as opposed to sidestream emissions from the burning/smouldering tip of the cigarette which do not emerge from the respiratory system). However, we emphasize that indoor exposure to ETS is much more hazardous than exposure to exhaled ECA in any aspect other than risk for SARS-CoV-2 virus transmission.

The section by section summary of the paper that illustrates its methodological structure is as follows. Background material is presented in section 2, which provides a brief summary of results of Sussman et al. (2020). In Methods I (section 3) we examine the visibility of exhaled ECA, commenting on its safety implications in section 7. In Methods II (section 4) we present a risk model of SARS-CoV-2 contagion in shared indoor spaces (home and restaurant scenarios, natural and mechanical ventilation) based on an adaptation and simplification of the model proposed by BMS (Buonanno et al. (2020a,b)). Our results on this risk model (without face mask wearing) are presented in section 5 (notice that face masks are seldom worn in a home scenario and compliance with this measure is lax in restaurant scenarios). A full discussion is provided in section 6 on the effect of face mask wearing, while safety considerations are discussed in section 7. The limitations and our conclusion are presented in sections 8 and 9.

2. Background

2.1. Respiratory droplets emission

In order to evaluate infection risks from vaping expirations in shared indoor spaces we need empiric data on relevant parameters of these expirations: tidal expired volume and characteristics of exhaled ECA carrying respiratory droplets, droplet emissions in such expirations and distances along which these droplets should be transported by them. As we argued in in Sussman et al. (2020), the lack of this data requires its inference through theoretical modeling guided by phenomena (on which this data exists) that can serve as proxies for vaping exhalations. Using this

inferred outcomes droplet propagation distances can be estimated through a model of a turbulent intermittent jet evolving into a puff.

In what follows we summarize the main results of the theoretical modeling undertaken in Sussman et al. (2020):

- **'Mouth to Lung' (MTL) low intensity vaping and smoking** The outcomes displayed in Table SM(2) and Table 2 of Sussman et al. (2020) suggest mean expired tidal volumes of $V_T = 700 - 900\,\mathrm{cm}^3$ potentially carrying $N_p = 6 - 200$ respiratory droplets per exhalation (mean $N_p = 79.82$, standard deviation 74.66), overwhelmingly in the submicron range (typically peaking at $d_p = 0.3 - 0.8\,\mu\mathrm{m}$) and droplet number densities well below $n_p = 1\,\mathrm{cm}^{-3}$. As shown in Figure SM(2) of Sussman et al. (2020), this is the style of vaping involving low powered devices practiced by 80-90 % of vapers in the main consumer markets (the US and the UK). However, the proxies we have used (cigarette smoking and mouth breathing) exhibit a wide individual variation in expired volumes, puffing parameters and droplet emission, all of which should occur also in vaping. Thus, the inferred data we have mentioned excludes the small minority of outlier individuals known as "super emitters" possibly emitting as much as $N_p \sim 1000$ respiratory droplets per exhalation in expired tidal volumes of up to 2 LT.

- **'Direct to Lung' (DTL) high intensity vaping**. It involves high powered tank devices that allow for a wider spectrum of deeper respiratory intensity than MTL vaping. It should involve a higher rate of droplet emission and expired volumes of 2-3 LT. Perhaps the closest analogue to infer its droplet emission rate among the studies listed in Table 2 of Sussman et al. (2020) is breathing at fractional residual capacity in Almstrand et al. (2010) that reported emission rates of around 1000/LT. However, this style of vaping is practiced by a small minority of vapers (roughly 10-20 %), with its upper end being extreme vaping (the so called "cloud chasers") that is only practiced in competitions or exhibitions. Evidently, this type of extreme vaping cannot be sustained for long periods and is not representative even of even DTL vapers.

While the inferred droplet numbers in the upper end of high intensity DTL vaping can be comparable with low end numbers for vocalizing, the latter involves modes with larger mean diameters because of distinct droplet generation processes Asadi et al. (2019); Morawska et al. (2009); Johnson et al. (2011).

2.2. Distance for direct exposure

The distance range that vaping expirations can transport respiratory droplets provides the spatial scope of direct pathogen exposure through exhaled ECA, modeled in Sussman et al. (2020) as an intermittent jet evolving as the exhalation ends into a turbulent puff. The scope of direct exposure is the displacement or penetration distance of the jet in the direction of the momentum of the jet at exhalation. The parameters characterizing the jet are expired tidal volume of air diluted ECA mentioned in section 2.1 and exhalation centerline velocities estimated in Sussman et al. (2020) as $U_0 = 0.5 - 3$ m/s (MTL vaping) and $U_0 = 1,5 - 5$ m/s (DTL vaping), which (assuming horizontal exhalation) yields a distance spread of 0.5-2.0 meters for the MTL vaping and over 2.0 meters for DTL. The maximal penetration goes beyond that afforded by the momentum trust of the starting jet, with the puff further evolving at lesser speeds. Before the puff stage centerline velocities drop to about 0.2 m/s at different times and distances when fluid injection stops in all cases.

Given its short time duration and close distance scope of the momentum trusted staring jet, the analytic model analyzed in Sussman et al. (2020) provides a reasonably good inference of the distance and direction that bystanders should keep to minimize the risk of direct exposure. As the jet evolves it mixes with surrounding air, with entrained air reaching about 40 % of the jet mass as exhalation (fluid injection) ends at the transition towards the puff regime Ghaem-Maghami (2006); Ghaem-Maghami and Johari (2010). Since at this point the jet velocities become comparable to typical velocities of $\sim$ 10 cm/s (and up to 25 cm/s) of airflow currents in home environments, even in still air with natural ventilation Matthews et al. (1989); Berlanga et al. (2017), the puff can be easily destabilized by vortex motion generated through turbulent mixing from the large velocity fluctuations produced by the entrainment Wei and Li (2015); Vuorinen et al. (2020).

Once the puff becomes disrupted bystanders face indirect exposure to mostly droplet nuclei, as submicron respiratory droplets evaporate almost instantly as they are exhaled (see Nicas et al. (2005)). Turbulence and thermal buoyancy and stratification become important factors when the jet initial momentum decreases, more so when the vaper (the source) moves or walks Wang and Chow (2011). Mechanical ventilation (mixed or displaced) He et al. (2011); Gao and Niu (2007); Gao et al. (2008) producing a faster disruption and dispersion of the slow moving puff through their own turbulent, thermal stratification and droplet dispersion patterns. In general, the dispersed submicron droplets and droplet nuclei can remain buoyant for hours, with mixing ventilation tending to uniformly spread them, whereas directed ventilation tends to stratify them along different temperature layers. The detailed description of droplet dispersion after the puff disruption is a complicated process that requires computational techniques that are beyond the scope of this paper (see comprehensive analysis in Vuorinen et al. (2020)).

3. Methods I: Visualization of the respiratory flow

As shown in Sussman et al. (2020), respiratory droplets that would be carried by exhaled ECA should be overwhelmingly submicron (just as ECA droplets). As a consequence, ECA droplets and the much fewer respiratory droplets accompanying them, should follow the fluid flow of ECA approximately as molecular contaminants, thus acting like visual tracers of the expiratory flow Ai et al. (2020); Nazaroff (2004). This visibility is shared with smoking (see Gupta et al. (2009, 2010); Ivanov (2019)), but is absent in other respiratory expirations (breathing, vocalizing, coughing, sneezing). It has important psychological and safety implications, since bystanders can instinctively detect (and avoid) the area of direct exposure. We provide here a brief discussion of optical properties of aerosols that allow for their visualization (see comprehensive explanation in Ruzer and Harley (2012); Hinds (1999); Kulkarni P and K (2011)).

Visualization and coloring of aerosols follow from the interaction of light with its particulate phase through absorption and scattering (refraction, reflection and difraction), which depends on the particles' number density n_p, chemical nature and the ratio of their diameters to visible light wavelengths: $\alpha = \pi d_p/\lambda$ with $\lambda = 0.4 - 0.7\,\mu$m. This interaction is described in relatively simple terms for ultra-fine particles ($d_p < 0.05\,\mu$m or $\alpha \ll 1$) by Rayleigh's molecular scattering theory and for large particles with $d_p > 100\,\mu$m in terms of geometric optics. Particles with diameters in the intermediate range correspond to Mie scattering theory, which becomes particularly complicated for d_p roughly comparable to λ or $\alpha \approx \pi$, as is the case for ECA and respiratory droplets. Since the latter are liquid droplets, they are in practice non-absorbing so that scattering is the dominant effect.

A simpler approach to aerosol optics follows from the notion of light extinction, the loss of intensity I from absorption and scattering in the direction of an incident parallel non-polarized light beam, with intensity I_0 and cross section distance L within an aerosol. This is described by the extinction coefficient σ_e through the Lambert-Beer (or Bouguer) law

$$I = I_0\, \mathrm{e}^{-\sigma_e L}, \qquad \sigma_e = \frac{\pi}{4} Q_e n \bar{d}^2, \tag{1}$$

where n is the total particle number density, $\bar{d}$ is the mean particle diameter and, for non-absorbing particles, $Q_e \approx Q_{\text{scatt}}$ is the scattering extinction efficiency taken as constant (a valid approximation for a fixed λ and a very small diameter range around $\bar{d}$).

The fact that n in non-biological aerosols (like exhaled ECA) is much larger than in bioarosols that are just "airborne" without ECA (as in "normal" respiratory activities) explains why exhaled ECA is visible while the bioaerosols are not. To illustrate this point quantitatively, consider the light extinction law (1) for an incident beam with wavelength $\lambda = 0.5\,\mu$m crossing an exhaled ECA jet (see figure 1 of Sussman et al. (2020)). From the mean diameters obtained in Sussman et al. (2020), we have $\bar{d} = \lambda = 0.5\,\mu$m and $\bar{d} = 0.4\,\mu$m for respiratory and ECA droplets (the latter just at exhalation before their rapid evaporation), while (from figure 16.2 of Hinds (1999)) we have $Q_e = 2$, 3.5 respectively for ECA and respiratory droplets, as their respective refractive indices are roughly those of water and VG: $m = 1.33$, 1.5. While L is the same (same fluid jet) and $\bar{d}$ and Q_e have comparable values for both types of droplets, the large difference in n makes a significant effect in light transmission through the beam that indicates the aerosol visibility in its specific direction if $I/I_0 < 1$. In numbers: we have $n_p \sim 10^7\,\mathrm{cm}^{-3}$ and $L = 15\,$cm for ECA just at exhalation, leading to impaired light transmission, $I/I_0 = 0.51$, while at 1 meter distance after significant dilution: $\bar{d} \sim 0.1$, $L = 25\,$cm and $n_p \sim 10^5\,\mathrm{cm}^{-3}$, we have almost full light transmission $I/I_0 = 0.99$. For respiratory droplets $n_p \sim 0.1 - 1\,\mathrm{cm}^{-3}$, leading to practically full light transmission $I/I_0 \approx 1$ irrespective of L (in the appropriate ranges delineated by the exhaled jet).

Extinction through a parallel beam provides a limited description of light scattering in an aerosol, which occurs through each droplet in all directions. The rigorous description through Mie scattering theory is beyond the scope of this paper, but it is evident that droplet numbers play a significant role since total scattered intensity is basically the sum of scattered intensity from each droplet. The light extinction law (1) is valid under the assumption that photons in all directions follow classical paths and their scattering complies with a Poisson distribution (a good approximation for sufficiently diluted aerosols). Under these assumptions the mean free path between scattering events is simply (see chapter 13 of Kulkarni P and K (2011)) $\ell = 1/\sigma_e = 1/(C_e\, n)$, where $C_e \propto \bar{d}^2$ is the extinction cross section per droplet. Evidently, light scattering in the scales of the ECA jet is negligible for bioaerosols with very low n, as the mean free path ℓ becomes extremely large (much larger than the bio-aerosol scale). For $\bar{d} = 0.5\,\mu$m, $Q_e = 2$ and $n \sim 0.1 - 1\,\mathrm{cm}^{-3}$ we have $\ell \to 10^8 - 10^9\,\mathrm{cm} = 10^3 - 10^4\,$km, a huge value that explains the practical lack of scattering events in these bio-aerosols.

4. Methods II: Risk model of contagion

Having considered the inferred data obtained in Sussman et al. (2020) on exhaled tidal volumes, emission rates, type of respiratory droplets and exhalation distance spreads, as well as the visibility of these exhalations, we need to evaluate exposure risks of bystanders sharing indoor

spaces with infected vapers. Specifically, we seek a model that takes into account exposure to SARS-CoV-2 viruses potentially carried by a total mass of droplet emission in indoor spaces irrespective of whether the exposure is direct or indirect. However, given the visibility of vaping (and smoking) exhalations, it is safe to assume that bystanders sharing indoor spaces with vapers will, extremely likely, avoid direct exposure to the exhaled jet and thus will be mostly subjected to indirect exposure to (mostly) droplet nuclei dispersed by surrounding air currents once the jet has become a puff subjected to thermal buoyancy and turbulent mixing. It is also important for a consistent risk model to examine viral exposure of a total mass of droplet emission for other expiratory activities (breathing, vocalizing, coughing, sneezing) under the same assumptions, though for these activities avoidance of direct exposure is not instinctive because the exhalations are not visible.

The data inferred in in Sussman et al. (2020) considered generic respiratory droplets without reference to a specific pathogen/disease and have not evaluated infection risks of exposed susceptible individuals. We undertake now this evaluation, referring specifically to the available information on the parameters of the SARS-CoV-2 virus, assuming as well that emitted respiratory droplets or droplet nuclei potentially carrying this virus have been dispersed uniformly throughout a given indoor micro-environment.

Besides visibility, another extremely important feature that fully characterizes exposure risks from vaping expirations is the significant shortening of exposure time because of their intermittent and episodic nature: an infectious vaper (symptomatic or not) would emit respiratory droplets only while vaping (120-200 daily exhalations Dautzenberg and Bricard (2015); Cahours and Prasad (2018)), whereas the same vaper will emit respiratory droplets continuously just by normal rest breathing (17,000–29,000 daily exhalations for 12-20 breaths per minute for healthy adults).

4.1. Infective quanta

To evaluate indirect exposure risks from vaping we simplify and adapt the analytic risk model of Buonanno, Morawska and Stabile (hereafter BMS) Buonanno et al. (2020a) who have examined the potential SARS-CoV-2 virus transmission in various indoor micro-environments (see also their previous paper Buonanno et al. (2020b)). BMS develop this model by means of Montecarlo simulations in which variability of droplet emission rates and exposure parameters is described by suitable probability distributions. Our approach is to assume median values for these variables (50 percentiles) of these distributions, similar to their approach in their previous paper Buonanno et al. (2020b). This is justified because our aim is to evaluate the risks from indoor COVID-19 transmission from vaping, speaking and coughing (all episodic or intermittent expirations) in comparison with what can be denoted as a "control case" scenario of risks in a space were the infectious vaper is only rest breathing (a continuous expiration). We are not aiming at providing a full comprehensive risk analysis for each respiratory activity separately under more realistic conditions (something that would justify a full separate study in itself).

BSM consider the notion of an infective "quantum": the dose of airborne respiratory droplet nuclei necessary to infect 63 % of exposed susceptible individuals. They introduce the "quantum emission rate" ER_q (emitted quanta per hour) for various respiratory expirations

$$\mathrm{ER}_q = \frac{c_v}{c_{\mathrm{RNA}}\, c_{\mathrm{PFU}}} \times f_{\mathrm{br}}\, V_T\, C_d, \tag{2}$$

where c_v is the viral load (RNA copies/mL) in the sputum of a SARS-CoV-2 infected person (symptomatic or not), c_{RNA} is the number of RNA copies per PFU (plaque forming unit) needed

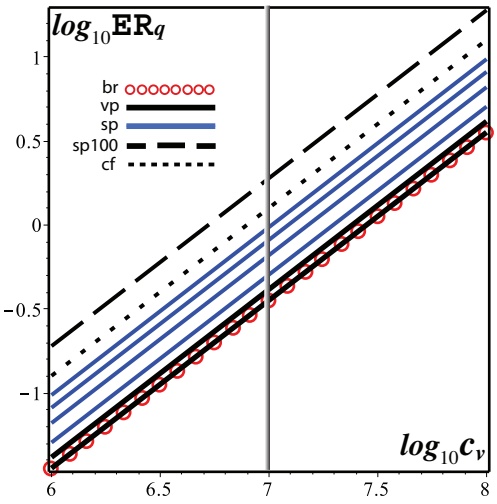

Figure 1: **Quanta emission rates.** The curves display $\mathtt{ER}_q$ (quanta/hour) as a function of viral load c_v (RNA copies/mL) for various expiratory activities: rest breathing (br), low and high intensity vaping (vp), speaking (bottom to top) 10, 20, 30, 40 % of the hour (sp), coughing (cf) and speaking 100 % of the time (sp100). Numerical values of $\mathtt{ER}_q$ for $c_v = 10^7$ RNA copies/mL (vertical line) are listed and discussed in the text. The ratios between these activities and rest breathing (taken as the case control scenario) is displayed in figure 4.

to generate infection and c_{PFU} is quanta-to-PFU conversion parameter, f_{br} is the number of breaths per hour and V_T the tidal exhaled volume, C_d is the droplet volume concentration (in mL/m^3, hence $C_d\, V_T$ is the total volume of exhaled droplets in mL). BMS define the product "$\mathit{IR} = V_T \times f_{\text{br}}$" as an "inhalation rate", but it can also be used as an exhalation rate expressible in units m^3/h.

For the infection parameters BMS consider values that have emerged from recent data: $c_v = 10^7$ RNA copies/mL (average in the range $10^3 - 10^{11}$), $c_{\text{RNA}} = 1.3 \times 10^2$ RNA copies/PFU and $c_{\text{PFU}} = 2.1 \times 10^2$ PFU/quanta. For the droplet volume concentration they take as reference an experimental value that incorporated dehydration effects in droplets associated with loud speech Stadnytskyi et al. (2020), then using experimental data from Morawska et al Morawska et al. (2009) to scale this reference to other respiratory expirations, leading to the following values (in mL/m^3)

$$C_d = 2 \times 10^{-2} \text{ (loud speech)}, \quad 6 \times 10^{-3} \text{ (normal speech)}, \quad 2 \times 10^{-3} \text{ (rest breathing)}, \tag{3}$$

In order to fit vaping expirations into these values we need to make some assumptions on the involved parameters, besides considering the effects on exposure from the time duration of expiratory activities. In particular, we need to evaluate their mean quanta emission rate *only* in the times when they occur and compare with the rates of normal rest breathing (which takes place all the time). To simplify matters, we assume that c_v, c_{I} and $f_{(\text{br})}$ are largely unaffected by the timing of these expiratory activities. We have then

- **Low intensity MTL Vaping**. A vaper breathes $N_{(\text{tot})}$ times in (say) one hour and of these breaths $N_{(\text{vp})}$ coincide with vaping expirations (puffs), the expression for $\mathtt{ER}_q$ in (2) must be

modified as

$$\mathtt{ER}_{q(\mathrm{vp})} = \frac{c_v\, f_{\mathrm{br}}}{c_{\mathrm{RNA}} + c_{\mathrm{PFU}}} \left[\frac{N_{(\mathrm{vp})}}{N_{(\mathrm{tot})}} V_{T\,(\mathrm{vp})}\, C_{d(\mathrm{vp})} + \left(1 - \frac{N_{(\mathrm{vp})}}{N_{(\mathrm{tot})}}\right) V_{T\,(\mathrm{br})}\, C_{d(\mathrm{br})} \right], \tag{4}$$

where $N_{(\mathrm{vp})}$ $N_{(\mathrm{tot})}$ are the number of vaping puffs and total number of breaths per hour, $V_{T(\mathrm{br})}$ $V_{T(\mathrm{vp})}$ and $C_{d(\mathrm{vp})}$, $C_{d(\mathrm{br})}$ are the tidal volumes and droplet volume concentration for vaping and rest breathing. For low intensity MTL vaping we assume a tidal volume of $V_T = 750\,\mathrm{cm}^3$ supported by data inferred and discussed in Sussman et al. (2020), while for droplet volume concentration we assume $C_d = 3 \times 10^{-3}\,\mathrm{mL/m}^3$, a plausible value denoting emissions slightly above rest breathing but below normal speech in (3), fitting the 'whispered counting' data of Morawska et al. (2009). For the number of breaths we can take the average values of 160 daily puffs in a 16 hour journey Dautzenberg and Bricard (2015); Cahours and Prasad (2018) and breathing frequency of $f_{(\mathrm{br})} = 16/\mathrm{min}$ (in the range 12-20), so that $N_{(\mathrm{tot})} = 960$ breaths/h and $N_{(\mathrm{vp})} = 10$ breaths/h.

- **High intensity DTL vaping**. We assume $V_T = 2000\,\mathrm{cm}^3$ as an average tidal volume. However, there is ambiguity in inferring a value for droplet volume concentration because of insufficient data on how much the larger tidal volume and deeper inhalation of DTL vaping can modify respiratory droplet numbers and diameters. As mentioned in section 2 of Sussman et al. (2020), higher powered devices associated with DTL vaping tend to increase ECA droplet sizes and diameters Lechasseur et al. (2019); Floyd et al. (2018) but it is not certain if this applies to respiratory droplets. However, as mentioned in section 3.3.2 of Sussman et al. (2020), speech involves droplet generating mechanisms that are distinct from those of breathing Asadi et al. (2019); Morawska et al. (2009); Johnson et al. (2011), resulting in higher rate of droplet emission even with a tidal volume only slightly larger than the breathing rest value of $400 - 600\,\mathrm{cm}^3$ Bailey and Hoit (2002); Hoshiko (1965). Thus, we have two plausible options to account for a higher total volume of exhaled droplets $\mathcal{V}_d = V_T\, C_d$: it may follow simply from a larger V_T with the same value $C_d = 3 \times 10^{-3}\,\mathrm{mL/m}^3$ of low intensity vaping, or we might assume the larger value of C_d for normal speech in (3). Instead of choosing one option, we will keep the continuous range of $C_d = 3 - 6 \times 10^{-3}\,\mathrm{mL/m}^3$. Regarding the number of breaths we can assume the same values as low intensity vaping: $N_{(\mathrm{tot})} = 960$ breaths/h and $N_{(\mathrm{vp})} = 10$ breaths/h.

- **Normal speech**. The equation for $\mathtt{ER}_q$ in (2) needs to be modified in a similar way as (4), replacing the droplet volume concentration C_d with the value for normal speech in (3) and we take as tidal volume the value $V_T = 600\,\mathrm{cm}^3$, roughly 10 % larger than the average rest value Bailey and Hoit (2002); Hoshiko (1965). To incorporate the timing we replace $N_{(\mathrm{vp})}$ with a number count of breaths coinciding with a given percentage of an hour interval spent on continuously speaking in a given indoor environmant. For 5, 10, 20, 30, 40 % of the hour (960 total breaths) we have $N_{(\mathrm{sp})} = 48, 96, 192, 288, 384$ breaths/h.

- **Coughing**. The emission data from coughing in Morawska et al. (2009) is comparable to that of 'unmodulated vocalization' (repeating the vowel "aahh"). Hence, we can use (4) with the value for droplet concentration volume of loud speaking in (3) as a proxy for coughing, while for coughing tidal volume we have $V_T = 1400\,\mathrm{cm}^3$ Gupta et al. (2009). Assuming a cough every 2 and 3 minutes, $N_{(\mathrm{vp})}$ is replaced by $N_{(\mathrm{cf})} = 20, 30$.

Considering the plausible assumptions stated above, we display in figure 1 the logarithmic plots of quanta emission rate $\mathtt{ER}_q$ from an infectious individual as a function of viral load c_v, for rest

breathing, low and high intensity vaping, speaking for 10 %, 20 %, 30 % and 100 % of the time, as well as coughing every 2 and 3 minutes. The numerical values of $\mathtt{ER}_q$ in quanta per hour for $c_v = 10^7$ RNA copies/mL are

$$\begin{aligned}
\mathtt{ER}_{q(\mathtt{br})} &= 0.3416, \quad \mathtt{ER}_{q(\mathtt{vpL})} = 0.3562, \quad \mathtt{ER}_{q(\mathtt{vpH})} = 0.3727 - 0.4139, \\
\mathtt{ER}_{q(\mathtt{sp10})} &= 0.5063, \quad \mathtt{ER}_{q(\mathtt{sp20})} = 0.6610, \quad \mathtt{ER}_{q(\mathtt{sp30})} = 0.8158, \\
\mathtt{ER}_{q(\mathtt{sp40})} &= 0.9705, \quad \mathtt{ER}_{q(\mathtt{cf})} = 1.2637, \quad \mathtt{ER}_{q(\mathtt{sp100})} = 1.8216,
\end{aligned} \tag{5}$$

where the symbols `br`, `vpL`, `vpH`, `sp10`, `sp20`, `sp30`, `sp40`, `sp100` and `cf` respectively denote breathing, vaping low and high intensity, speaking 10, 20, 30, 40, 100% of the hour and coughing 30 times. Notice that for low and high intensity vaping $\mathtt{ER}_q$ is very close to the control case of rest breathing (almost indistinguishable for low intensity vaping), while even speaking 10 % of the hour (6 minutes) yields a larger $\mathtt{ER}_q$ value than the upper end of high intensity vaping. Also, normal speech for a full hour (not uncommon) produces a higher quanta emission than coughing 30 times

4.2. Exponential dose-response risk model

In order to evaluate a time dependent risk for expiratory activities that incorporates quanta emission rates and indoor environment variables, BSM consider the "dose response exponential model" given in terms of the the density of the quanta $n(t)$ in units quanta/m^3 under the assumption that $n(0) = 0$ (no exposure at initial time $t = 0$)

$$R = 1 - \exp\left[-\mathtt{IR} \int_0^T n(t)\, dt\right] = 1 - \exp\left[-\frac{\mathtt{IR}\,[\mathtt{ER}_q\, N\, T - n(T)\, V]}{\mathtt{IVVR}\, V}\right], \tag{6}$$

$$n(t) = \frac{\mathtt{ER}_q\, N}{\mathtt{IVVR}\, V}\left[1 - \exp(-\mathtt{IVVR}\, t)\right], \tag{7}$$

where V is the volume (m^3) of the indoor micro-environment, N is the number of exposed susceptible individuals, $\mathtt{IR}$ is the inhalation rate (m$^3/h$) of these individuals and $\mathtt{IVVR}$ is the infectious virus removal rate, which which BMS take as the sum of three factors: $\mathtt{IVVR} = \mathtt{AER} + \kappa + \lambda_0$, where $\mathtt{AER}$ is the ventilation air exchange rate, κ is the particle deposition on surfaces and λ_0 is the virus inactivation (all of these quantities given as h^{-1}).

We evaluate in section 5 the risk R for vaping exhalations and other respiratory activities, aiming at the evaluation of their relative risk with respect to the control state of continuous breathing, assuming a home and restaurant scenarios with natural and mechanical ventilation.

5. Results I: Risk evaluation

To evaluate the risk of exposure to respiratory droplets carried by vaping exhalations in indoor environments we have adapted in section 4 the "dose response exponential model" developed by Bounnano, Morawska and Stabile (BMS) Buonanno et al. (2020a) [1] . Specifically, we evaluate equation (6) that defines the risk R (as a fraction < 1) for the value $\mathtt{IR} = 0.96$m^3/h taken from the previous paper of BMS Buonanno et al. (2020b) and justified as a level of physical activity half way between standing and light activity. For the remaining parameters BSM assume the range

[1] We do not assume face mask wearing in this subsection. Effects of face masks are discussed in section 6.

$\texttt{AER} = 0.2 - 0.5/h$ for natural ventilation and $\texttt{AER} = 9.6/h$ for a restaurant scenario with mixed ventilation. BMS compute the deposition rate by dividing typical gravitational settling velocity for supermicron particles (10^{-4} m/s) by the height of emission (1.5 m), leading to $\kappa = 0.24/h$, while for the viral inactivation they take the measured aerosolized SARS-CoV-2 virus mean life of 1.1 hours Van Doremalen et al. (2020) and even longer periods Fears et al. (2020), leading to $\lambda_0 = 0.63/h$. We consider the following home and restaurant indoor scenarios:

- Home scenario. We assume one infectious vaper and three exposed susceptible family members ($N = 3$). Total exposure time $T = 12$ h. Indoor volume 125 m^3 (small 50 m^2 apartment with roof height of 2.5 m). For natural ventilation: $\texttt{AER} = 0.2/\text{h}$ we have $\texttt{IVVR} = 1.07/\text{h}$.

- Restaurant, natural ventilation with open door. Thirty costumers ($N = 30$), total exposure time $T = 3$ h. Air exchange rate $\texttt{AER} = 0.5/\text{h}$, indoor volume 300 m^3 (100 m^2 area with roof height of 3 m), results in $\texttt{IVVR} = 1.37/\text{h}$

- Same restaurant endowed with mechanical ventilation: $\texttt{AER} = 9.6/\text{h}$ (taken from Buonanno et al. (2020b)), results in $\texttt{IVVR} = 10.47/\text{h}$

The infection risk R for home and restaurant scenarios is plotted in figures 2 and 3 as a function of time for breathing, low and high intensity vaping, various percentages of time spent speaking and coughing every 2 minutes, considering natural and mechanical ventilation. As expected from the quanta emission rates displayed in figure 1, the exposure time of different expirations is a crucial factor in computing R. As expected, the risk factor R increases with exposure time T, displaying an approximately growing linear dependence that keeps the same shape but is is markedly decreased with mechanical ventilation in in each scenario: R decreases to one third (25 % to 8 %) after 12 hours exposure in a home environment with air exchange rate of 3/h and one fifth (25 % to 5 %) after 3 hours exposure in a restaurant environment with air exchange rate of 9.6/h. However, the key point is not the absolute values of $R(T)$ but its comparison for various respiratory activities and the control state of exclusive normal rest breathing. Figures 2 and 3 reveal that exposure to vaping expiration (vaper doing 10 puffs per hour) poses an infection risk to bystanders that is very close to that from the control case scenario. In fact, for low intensity vaping the infection risk $R(T)$ is practically indistinguishable from the control case and even for high intensity vaping it is well below that from the same person speaking and coughing. Speaking only for 10 % of the time (6 minutes per hour) already yields a higher infection risk than high intensity vaping, while speaking $30 - 40$ % of the hour yields up tp 4 times the infection risk, which is roughly the values plotted in figure 4.

A good inference of the risk from intermittent and episodic expiratory activities (vaping, speaking, coughing) relative to the control case scenario of exclusive rest breathing (a continuous expiration) is furnished by the ratio $R_{(\text{A})}/R_{(\text{br})}$, where $A = \text{vp}, \text{sp}, \text{cf}$ (see (5)). Plotting this ratio from (6)–(7) for every expiratory activity yields near constant curves around the values of the quotients $\texttt{ER}_{q(\text{A})}/\texttt{ER}_{q(\text{br})}$ (see numerical values in (5)). This is not surprising since $\texttt{ER}_q$ is the only variable in R that characterizes the infectious person (the other variables characterize the indoor micro-environment and the exposed susceptible persons). Hence, given the same indoor micro-environment and same number of susceptible individuals, we consider risks relative to the control case scenario of rest breathing in terms of the ratio of quanta emission. Using (4) we have

$$\varepsilon = \frac{\texttt{ER}_{q(\text{A})}}{\texttt{ER}_{q(\text{br})}} = 1 + \left(\frac{\mathcal{V}_{d(\text{A})}}{\mathcal{V}_{d(\text{br})}} - 1 \right) \approx \frac{R_{(\text{A})}}{R_{(\text{br})}}, \tag{8}$$

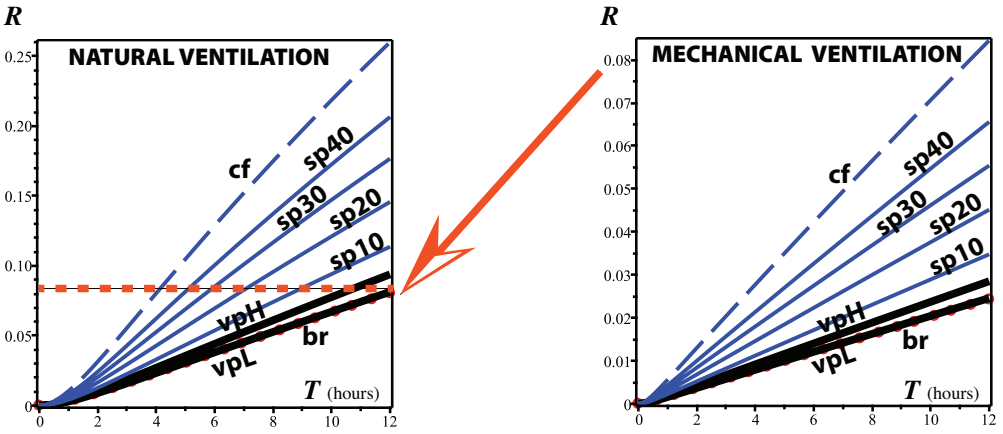

Figure 2: **Infection risk in a home environment.** The curves display R as a function of exposure time T from (6). The abbreviations br, vpL, vpH, sp10, sp20, sp30, sp40 and cf stand for rest breathing, vaping low intensity, vaping high intensity (upper end option), speaking for $10, 20, 30, 40, \%$ of time and coughing. Notice the dramatic reduction of R achieved by mechanical ventilation (moderate air exchange rate of $3/\text{h}$). Also: the curves for the risks from vaping (full range of intensities) are practically indistinguishable from that of the case control scenario of rest breathing (red circles).

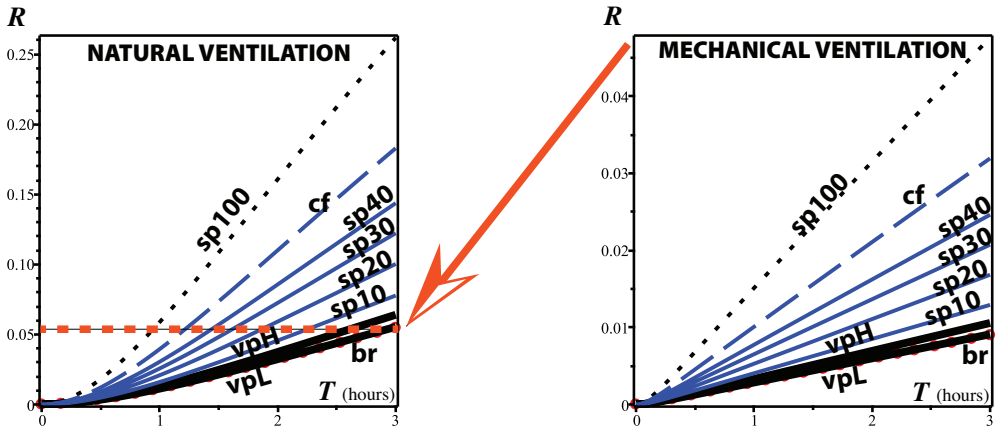

Figure 3: **Infection risk in a restaurant.** The same abbreviations as in figure 2 plus sp100 (speaking 100 % of the time, a possible outcome when spending 3 hours in a restaurant). As in figure 2, mechanical ventilation (air exchange rate $9.6/\text{h}$) achieves a dramatic reduction of R and the curves for the risks from vaping are practically indistinguishable from the curve of the control case scenario of rest breating (red circles).

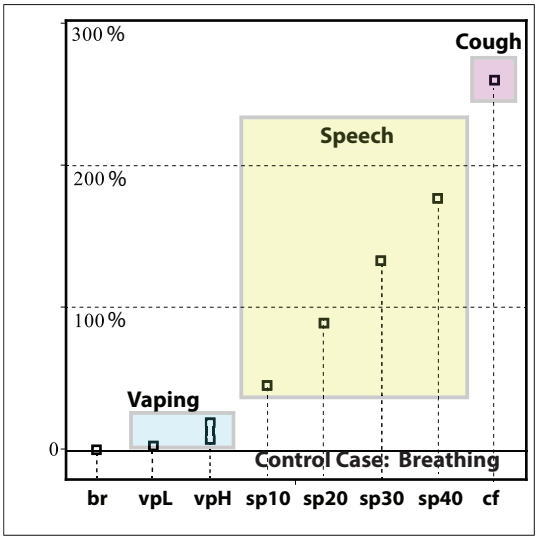

Figure 4: **Added percentage risks of expiratory activities with respect to the control case scenario of rest breathing.** The percentage values with respect to the control case are: low intensity vaping 1.3 % (vpL), high intensity vaping 5.2-17.7 % (vpH), speaking 44% (sp10), 88% (sp20), 132% (sp30), 176% (sp40) for 10%, 20%, 30%, 40% of time, coughing 259% 30 times per hour (cf). These values were obtained from $(\varepsilon - 1) \times 100$ for ε defined for these expiratory activities by (8)–(10).

where $\mathcal{V}_{d(\mathrm{A})} = V_{T(\mathrm{A})} C_{d(\mathrm{A})}$ is the total exhaled droplet volume (in mL) for each expiratory activity "A". Since $N_{(\mathrm{br})} = N_{(\mathrm{tot})}$, then for a heavy breathing activity in intense aerobic exercise ε might grow only because of the much larger tidal volume. However, for a truly intermittent expiration like vaping we have $N_{(\mathrm{vp})}/N_{(\mathrm{br})} \ll 1$ and thus $\varepsilon \approx 1$ holds even if we have $\mathcal{V}_{d(\mathrm{A})}/\mathcal{V}_{d(\mathrm{br})} \gg 1$ (large exhaled amount of droplets as with the large tidal volumes in extremely intense vaping). For the values of tidal volume and droplet volume concentration we have used the numerical values in (5), we have the following relative risks

$$\varepsilon = 1.25 \times \frac{N_{(\mathrm{vpL})}}{N_{(\mathrm{br})}} \ \text{(low intensity vaping)}, \quad \varepsilon = 5 - 11 \times \frac{N_{(\mathrm{vpH})}}{N_{(\mathrm{br})}} \ \text{(high intensity vaping)}, \tag{9}$$

$$\varepsilon = 3.6 \times \frac{N_{(\mathrm{sp})}}{N_{(\mathrm{br})}} \ \text{(speaking)}, \quad \varepsilon = 28 \times \frac{N_{(\mathrm{cf})}}{N_{(\mathrm{br})}} \ \text{(coughing)}, \tag{10}$$

which provides an intuitive indication of the added exposure risks relative to the control case from the different expiratory activities.

We display in figure 4 the numerical values of ε, as an added risk with respect to the control case for various expiratory activities with respect to the continuous presence of risk from rest breathing and under the assumptions we have used. These numbers clearly reflect the effects of the intermittence or duration time of each activity. Under normal vaping conditions (10-15 puffs per hour) the added risk of low intensity vaping respect to the control scenario of exclusive rest breathing is of the order of ~ 1 % (since $\varepsilon - 1 \sim 10^{-2}$). For high intensity vaping it is $\sim 5 - 17$ %, given the ambiguity in the range of $\mathcal{V}_d = V_T C_d$, still it is of the order of $\varepsilon - 1 \sim 5 \times 10^{-2} - 10^{-1}$, also a low added risk since the low value of $N_{(\mathrm{vp})}/N_{(\mathrm{br})}$ compensates for the large exhaled tidal volume.

Notice that the added risk respect to the control case grows to $\sim 40\,\%$ just for talking for $10\,\%$ of the time and easily reaches $176\,\%$ if talking $40\,\%$ of the time. Coughing is also intermittent, possibly even more intermittent than vaping, but its large amount of exhaled droplets (large factor of 28 in (10)) can offset this effect. For speaking ε can be large even if normal speech involves a tidal volume close to rest breathing, but it also involves a much larger amount of time (larger number of breaths in typical conversation).

6. Discussion I: Effects of face mask wearing

In our risk evaluation in a home and restaurant scenarios in section 5 we did not assume face mask wearing by emitters and receivers of infective quanta. However, this fact has little real life relevance in our risk evaluation for the home scenario because face mask are rarely worn at home (even under confinement). Assuming that containment measures permit that bars and restaurants remain open, our risk evaluation also remains roughly valid for such venues (if vaping is allowed), even if vaping necessarily requires the vaper to remove the face mask (at least for the brief time lapse of intermittent puffs). In fact, eating and drinking in a restaurant scenario also require face mask removal, which in a convivial atmosphere (with conversations accompany eating and drinking) should involve quanta emissions by mask-free patrons whose duration is likely to exceed the strict time needed to eat and drink. However, it is still necessary to examine exposure risks in hypothetical indoor scenarios in which universal face mask wearing is strictly enforced. In particular, we need to emphasize the effects on those face masks that are usually worn at a community level: surgical masks and/or those made of cotton and other fabrics.

Face masks, in their multiple designs and fiber characteristics (see review in Tcharkhtchi et al. (2020)), filter aerosol particles through various physical processes: gravitational sedimentation, inertial impaction, interception, diffusion and electrostatics, each of which govern and/or becomes dominant in specific ranges of particle sizes, airflow, leaks and environmental factors according to aerosol filtering theory (see Hinds (1999)). The key issue we need to assess is how much cotton and surgical masks protect (in terms of filtering efficiency) their wearers from *inward* emission when they are exposed to *outward* quanta emissions by potentially infectious individuals not wearing face masks (as vapers when vaping). It is especially useful to compare this protection with respect to the one they would get when exposed to emitters who are also masked (*i.e. reciprocal masking*).

Filtering efficiency is high in outward emission for N95 respirators (over $90\,\%$) and slightly less so ($74\,\%$) in surgical masks in human emitters breathing, speaking and coughing Asadi et al. (2020), with decreasing diameters of filtered droplets, though in these experiments droplet counts excluded ultra-fine droplets below $0.3\,\mu$m and leaks were not evaluated. Similar results were obtained in laboratory conditions with a non-biological aerosol, though leaking decreased efficiency in surgical and cotton masks between one half and two thirds Drewnick et al. (2021).

Evidently, face masks also protect their wearers from inward emissions, as revealed by the following two laboratory experiments:

- In Sickbert-Bennett et al. (2020) two human subjects in different body postures, wearing well fit N95 respirators and surgical masks (tied with stripes or ear loops), were exposed to a non-biological polydisperse aerosol ($d_p = 0.02 - 3.00\,\mu$m) released in a chamber at concentrations between 2000-5000 cm^{-3}. Fitted filtration efficiency was above $95\,\%$ in all N95 respirators, $71.5\,\%$ for the surgical mask tied with stripes and $38.1\,\%$ for the one fit

with ear lobes. Efficiency decreased for the latter to 21.2 % when the subjects turned their head left or right, showing the effects of leaks.

- In Ueki et al. (2020) a bio-aerosol generated by a nebulizer emitted at flow velocity of 2 m/s, simulating a mild cough airflow, was used to examine virus penetration (in terms of virus titer) between two mannequins separated at distances of 50 and 100 cm, in experiments wearing loose and fit N95 respirators, surgical and cotton masks. The filtering efficiency was measured in terms of the detected percentage of virus titer in the receiving mannequin with respect to the titer in the emitting one. For 10^5 PFU (plaque forming units) when the receiver was wearing different face masks and the emitter was unmasked filtering efficiency was: 17 %, 47 %, 57 % and 79 % for the cotton mask, surgical mask, loose and fit N95 respirators respectively. When both mannequins wore a surgical mask the filtering efficiency significantly rose to 60 %, 71 %, 69 % and 92 %. Efficiency was about 10 % lower for 10^8 PFU. Virus titers decreased to 45 % and 31 % when mannequins (both unmasked) were placed at distances of 50 cm and 100 cm with respect to their values at 25 cm separation.

Both laboratory experiments describe, in spite of their idealization, the relatively low protection afforded by cotton and surgical masks to bystanders exposed to either unmasked emitters at close range and/or high droplet concentrations, flow and virus titer, which are precisely the conditions characteristic of direct exposure that would likely affect bystanders (wearing such masks) placed at the source (close to the mouth) and in the direction of the jet exhaled by an infectious vaper or by someone infectious breathing, talking or coughing without wearing a mask.

However, as opposed to masked bystanders exposed to mask-less emissions from other respiratory activities, we showed in section 3 that bystanders close to a vaper in shared indoor spaces can avoid instinctively the spatial zone of direct exposure that is clearly delineated by the visible emission jet exhaled by a vaper. These are evidently very different exposure conditions from those of the experiments described above, as bystanders wearing cotton or surgical masks located outside the exhaled jet would be subjected only to indirect exposure to a very low concentration of submicron droplet nuclei dispersing through air currents at ambient velocities that depend on the ventilation regime (roughly below 10-20 cm/s with natural ventilation Matthews et al. (1989); Berlanga et al. (2017)). In fact, the role and scope of SARS-CoV-2 transmission through indirect exposure to these submicron droplets and droplet nuclei (what the WHO and most medical literature denotes as "aerosols") is still uncertain and controversial NAS (2020); Jayaweera et al. (2020); Shiu et al. (2019); Sommerstein et al. (2020).

In particular, a much decreased airflow in indirect exposure implies a much decreased face velocity U_f, the air velocity at the mask surface obtained by dividing the air flow (LT/min) over the mask surface area. For the range of flow of rest breathing 10-25 LT/min, we have $U_f = 6 - 12$ cm/s (see Drewnick et al. (2021)), which is qualitatively analogous to characteristic velocities of indoor circulation currents with natural ventilation. Intuitively, under these low intensity flow conditions the masks capture more particles (droplets and nuclei) because the permanence time of the latter favors the capture mechanisms that are dominant for the particle diameter $d_p > 0.3\,\mu$m: inertial impaction and interception. The dependence of the percentage of filtration efficiency E on U_f when these mechanisms are dominant is given by $E \propto [1 - \exp(-U_f^{-4/9})] \times 100$ for a broad range of filtering parameters (see equations 9.19 and 9.35 of Hinds (1999)), which for $d_p > 0.3\,\mu$m yields $E > 90\,\%$ (see figures 9.9 and 9.10 of Hinds (1999)). The same arguments should apply to indirect exposure to drifting droplet nuclei from other respiratory activities that are sufficiently small to remain buoyant for long times.

As a consequence, universal wearing of cotton and surgical face masks offers a significantly higher level of protection against indirect exposure to small droplets and nuclei spread once respiratory droplets have evaporated. Evidently, it would be extremely complicated to adapt the relative risk model we have presented in section 4 to these conditions, since we would have to re-calculate in terms of the filtering efficiency of the face masks the quanta emission assigned to the control state of breathing emitters, of the comparative emitters talking and coughing, as well as the exposed receivers. However, incorporating this complexity might not be worthwhile after all, given the fact that the added contribution of vaping to the overall respiratory droplet emission from the control state of breathing remains vary small.

7. Discussion II: safety considerations

The results of our analysis, as listed in detail in section 5 and figures 2, 3 and 4, reveal that vaping expirations (by being intermittent and with low emission rates close to breathing) represent a minor risk increase of exposure to SARS-COV-2 transmission with respect to the control state: low intensity vaping (practiced by 80-90 % of vapers) involves a 1 % increase of the risk while high intensity vaping involves an increase of risk of 5-17 % (the uncertainty follows from the lack of a precise inference on its droplet emission rate). As a comparison (see figure 4) speaking 6-24 minutes per hour increase the risk by 44–176 % and coughing 2 times per minute in an hour by 259 %.

It is worth remarking that exposure time and ventilation modify the (approximately linear) dependence of infective risk R exposure time T, but keeps the comparative relative risks plotted in figure 4 roughly constant. This is consistent with the fact that figures 2 and 3, which display $R(T)$ for the various respiratory activities under natural and mechanical ventilation for the same micro-environment conditions (under the parameters used by BMS), show that the slopes for vaping (low and high intensity) in all cases are practically indistinguishable with the slope for the the breathing control state.

As mentioned in the introduction, there is an ongoing controversy on whether available evidence favors as main aerial COVID-19 contagion factor direct exposure to "droplets" (droplets with $d_p > 5\,\mu$m) or indirect exposure to "aerosols" (small droplets and droplet nuclei $d_p < 5\,\mu$m) (see NAS (2020); Jayaweera et al. (2020); Shiu et al. (2019); Sommerstein et al. (2020)). Although respiratory droplets potentially carried by exhaled ECA are well within the range of "aerosols", this controversy has practically no effect for the risk evaluation we have undertaken, since our goal has been the evaluation of relative risks of respiratory activities in comparison with a well defined control state of pure breathing. Evidently, the latter control state and the values of the parameters used to compute risk of infection $R(T)$ for all respiratory activities might change if either one of "aerosols" of "droplets" become the dominant factor, but this would roughly affect all respiratory activities in similar ways, which suggests that the relative risks we have computed are likely to keep roughly the same proportionality to the control state.

7.1. Safety considerations from the flow visualization

As shown in section 3, vaping expirations potentially carrying the SARS-CoV-2 virus are visible (as opposed to other respiratory activities). Besides the evident psychological dimension of this flow visualization, there are safety implications: vapers and those surrounding them have a clear, instinctive and immediate delineation of the flow's horizontal and vertical distance reach and spreading direction along the exhaled jet. From the outcomes of the hydrodynamical analysis carried in Sussman et al. (2020), we can recommend as a basic safety measure to avoid direct

exposure (irrespective of face mask wearing) by keeping a 2 meter distance away from the vaper (when vaping) in the direction of the visible jet. However, notice that exhalation ranges above 2 meters are unusual, as 80-90 % of vapers use low powered devices whose exhaled jets reach well below 2 meters (and typically exhaling with a 30 degrees downward angle, see Sussman et al. (2020)). In other directions away from the jet (even at close distance) the exposure is indirect, but nevertheless as a safety measure it is prudent to maintain 2 meters of separation in all directions from anyone vaping when not wearing a face mask. Notice that these recommended safety measures coincide with the standard social separation recommendations adopted worldwide Hsiang et al. (2020).

7.1.1. Face masks.

In computing exposure risks in section 5 we did not consider face mask wearing. This is justified because face masks are not usually worn in a home scenario. Even in a restaurant or bar scenario, patrons are likely to remain mask-less for extended periods because masks must be removed for eating and drinking (as with vaping). As we discuss in section 6, face masks of common usage (surgical and cotton) afford limited protection to bystanders wearing them subjected to direct exposure to respiratory droplets from mask-free emitters. However, once outside the direct exposure zone (visible and delineated for vaping), bystanders wearing common usage face masks would be effectively protected from indirect exposure to dispersing droplets or nuclei with diameters above $0.3\,\mu$m remaining buoyant for extended periods.

7.1.2. Lockdown vs opening.

Risk assessments are essential to provide evidence based support for preventive and mitigating policies that have been proposed and enacted worldwide (see review Hsiang et al. (2020)). These assessments are sensitive to the wide variety of rapidly changing pandemic conditions and scenarios. High levels of severity characterized by frequent contagion rates can be addressed by lockdowns contemplating different levels and stages of home confinement. Under these conditions the risk assessment for the home scenario that we presented is particularly relevant, as a large number of vapers and smokers become home bound for a range of large periods. As we argue in Sussman et al. (2021), the risk assessment undertaken in the present paper provides valuable information for safety policies in this scenario: low intensity vaping only produces a minuscule ($\sim 1\,\%$) extra contagion risk with respect to the control case scenario of continuous breathing. Safety interventions should consider that abstention from vaping would not produce a noticeable safety improvement, but could generate an undesired level of stress and anxiety under long term confinement. High intensity vaping produces a higher increase of relative risk, but still well below speaking and coughing. Notice that face masks are seldom worn in home bound scenarios of family clusters.

8. Limitations

Lack of empiric data. Given the lack of experimental and observational data on respiratory droplets carried by exhaled ECA, we had to consider as basic input for the risk model the data inferred in Sussman et al. (2020) on the basis of theoretical speculation from the physical and chemical properties of ECA and extrapolation from available data on other expiratory activities (cigarette smoking and mouth breathing with a mouthpiece) that can serve as reasonable proxies for vaping. Evidently, the present paper inherits another important limitations of Sussman et al.

(2020): the oversimplification of vaping styles by classifying a complex usage pattern into two categories, "low" and "high" intensity" vaping, which cannot capture the full range and scope of individual vaping habits.

*Oversimplification of infective parameters and individual variability.*The rates of emitted droplets inferred for vaping are rough average estimates gathered from outcomes reported in breathing studies (see Table 2 of in Sussman et al. (2020)), involving a wide variety of subjects, including both healthy and individuals affected by respiratory conditions (not by SARS-CoV-2). Also, we did not considered the small minority of outlier individuals who are super spreaders emitting significantly larger numbers of droplets Asadi et al. (2019). Also, the data on infective SARS-CoV-2 parameters gathered by BMS that we use in section 4 is also subjected to uncertainties that they specifically recognize. In fact, numerous aspects associated with the spreading and infection details of the SARS-CoV-2 virus remain uncertain and subject to large (often unexplained) individual and environmental variability (a good summary of these uncertainties is found in Klompas et al. (2020); Morawska and Milton (2020); Morawska and Cao (2020); NAS (2020)). However, in order to be able to model a possible (previously unexplored) route of droplet transmission and possible infection, it is necessary and unavoidable to simplify this complexity and lack of data to obtain plausible order of magnitude estimates that can be verified once empiric evidence is available.

Oversimplification of the risk model. The adapted BMS risk model that we presented in section 4 is also simplified. While it fulfills our aim of providing a rough comparative estimation of relative risks with respect to the control case of continuous rest breathing, we do recognize its limitations: the risks are evaluated for a single vaper in highly idealized micro-environments, assuming constant infection parameters and inhalation rates (which BMS also assume), ignoring as well probability distributions of the quanta emission rates that convey individual variation on infection susceptibility and other parameters (which the model of BMS does incorporate). A more elaborate and complete approach should include a more robust methodology to quantify exposure risks to intermittent and sporadic sources, as for example in Nazaroff (2004); Ai et al. (2019). This task is left for a future analysis.

9. Conclusion

We have presented in this paper a risk analysis of COVID-19 contagion through direct and indirect exposure to the SARS-CoV-2 virus potentially carried by respiratory droplets and droplet nuclei that would be carried by ECA (e-cigarette aerosol) exhaled by vapers in shared indoor spaces (home and restaurant scenarios). This risk analysis is based on suitable adaptations of the risk model presented by BMS (see Buonanno et al. (2020a,b)) that incorporates experimental data on SARS-COV-2 infective quanta: we consider vaping expirations characterized by the respiratory parameters inferred in Sussman et al. (2020), we also considered the quantitative effects of exposure from the characteristic duration times of vaping and of other expiratory activities (breathing, vocalizing and coughing). In particular, given the fact that breathing is a continuous (and unavoidable) expiratory activity, we considered the rate of infective quanta of pure breathing (without vocalizing, coughing or vaping) as a "control state" that serves as reference to evaluate comparative risks for the rest of the inspiratory activities. To complement this risk analysis we also discussed the visibility of vaping expirations (section 3) and the usage of face masks in the indoor scenarios under consideration (section 6).

Vaping expirations represent a minimal increase of risk with respect to continuous breathing in home and restaurant scenarios with natural and mechanical ventilation (1 % and 5–17 %

for low and high intensity vaping). Visibility of vaping expirations is protective, as it allows avoidance of the high risk of direct exposure to droplets and droplet nuclei potentially carrying the SARS-CoV-2 virus. Those sharing indoor spaces with vapers do not require extra safety interventions besides those already recommended for the general population: wearing face masks and keeping a separation distance of 1.5-2 meters to avoid direct exposure. Setting aside harms from environmental tobacco smoke unrelated to COVID-19, these recommendations should also apply to sharing an indoor space with a smoker.

List of abbreviations and symbols

Acronyms and abbreviations

ECA, E-Cigarette Aersosol

COVID-19 Coronavirus disease 2019

SARS-CoV-2 Severe acute respiratory syndrome coronavirus 2

BMS Bounnano, Morawska & Stabile

MTL Mouth to Lung (vaping style)

DTL Direct to Lung (vaping style)

RNA Ribonucleic acid

PFU Plaque forming units

br Breathing

vp Vaping

vpL Vaping low intensity

vpH Vaping high intensity

sp10 Speaking 10% of time

sp20 Speaking 20% of time

sp30 Speaking 30% of time

sp40 Speaking 40% of time

sp100 Speaking 100% of time

cf coughing

Units

LT Litters

mL mililitters

m meters

cm centimeters

μm micrometers

s seconds

h hour

Variables

V_T Tidal volume

N_p Number of particles

d_p Diameter of particles

n_p Number of particles

U_0 Exhalation velocity

α diameter to wavelength ratio

L Cross section distance within the aerosol

λ light wavelength

I Beam intensity

I_0 Incident beam intensity

σ_c Extinction coefficient

Q_c Scattering extinction coefficient

$\bar{d}$ Mean particle diameter

ℓ Mean free path between scattering events

ER_q Quanta emission rate

c_v Viral load (RNA copies per mL)

c_{RNA} Number of RNA copies per PFU

c_{PFU} Quanta to PFU conversion parameter

f_{br} Number of breaths per hour

C_d Droplet volume concentration ($\mathrm{mL/m^3}$)

721 `IR` Inhalation rate

722 $N_{(\text{tot})}$ Total number of breaths per hour

723 $N_{(\text{vp})}$ Number of breaths/puffs per hour for vaping

724 $N_{(\text{sp})}$ Number of breaths per hour while speaking

725 $\mathcal{V}_d$ Total volume of droplets

726 R Risk for expiratory activities

727 T Exposure time

728 n Density of quanta

729 N Number of exposed susceptible individuals

730 V Volume of indoor space

731 `IVVR` Infective virus removal rate

732 `AER` Air Ventilation exchange rate (per hour)

733 κ Particle deposition on surfaces (per hour)

734 λ_0 virus inactivation (per hour)

735 U_f Face velocity

736 E Efficiency of filtration

737 **Declarations**

738 Ethics approval and consent to participate

739 Not applicable

740 Consent for publication

741 Not applicable

742 Availability of data and materials

743 Not applicable

744 Competing interests

745 RAS has no competing interests to declare.

746

747 EG is currently employed by Myriad Pharmaceuticals, an independent company that man-
748 ufactures e-liquids and vaping devices in New Zealand. She also provides consultancy
749 work on research and development, regulatory affairs support, and formulation to several
750 independent vaping companies in the Pacific Region. In the past she has worked for several
751 pharmaceutical companies, including GlaxoSmithKline and Genomma Lab. She is also a

member of the standards committee of the VTANZ and UKVIA.

RP is full time employee of the University of Catania, Italy. In relation to his work in the area of tobacco control and respiratory diseases, RP has received lecture fees and research funding from Pfizer, GlaxoSmithKline, CV Therapeutics, NeuroSearch A/S, Sandoz, MSD, Boehringer Ingelheim, Novartis, Duska Therapeutics, and Forest Laboratories. He has also served as a consultant for Pfizer, Global Health Alliance for treatment of tobacco dependence, CV Therapeutics, NeuroSearch A/S, Boehringer Ingelheim, Novartis, Duska Therapeutics, Alfa-Wassermann, Forest Laboratories, ECITA (Electronic Cigarette Industry Trade Association, in the UK), Arbi Group Srl., and Health Diplomats. RP is the Founder of the Center of Excellence for the acceleration of Harm Reduction at the University of Catania (CoEHAR), which has received a grant from Foundation for a Smoke Free World to develop and carry out 8 research projects. RP is also currently involved in the following pro bono activities: scientific advisor for LIAF, Lega Italiana Anti Fumo (Italian acronym for Italian Anti Smoking League) and Chair of the European Technical Committee for standardization on Requirements and test methods for emissions of electronic cigarettes (CEN/TC 437; WG4).

Funding

This research did not receive any specific grant from funding agencies in the public, commercial, or not-for-profit sectors.

Author contributions

Conceptualization, EG and RAS and; methodology, RAS.; investigation, RAS, EG and RP.; resources, RAS, EG and RP ; writing-original draft preparation, RAS, EG and RP writing-review and editing, RAS, EG and RP.; visualization, RAS and EG.; All authors have read and agreed to the published version of the manuscript. RAS (Roberto A Sussman), EG (Eliana Golberstein), RP (Riccardo Polosa).

Acknowledgements

None

References

, 2020. Airborne Transmission of SARS-CoV-2: Proceedings of a Workshop in Brief. National Academies of Sciences, Engineering, and Medicine, The National Academies Press, Washington, DC.

Ai, Z., Hashimoto, K., Melikov, A. K., 2019. Airborne transmission between room occupants during short-term events: Measurement and evaluation. Indoor air 29 (4), 563–576.

Ai, Z., Mak, C. M., Gao, N., Niu, J., 2020. Tracer gas is a suitable surrogate of exhaled droplet nuclei for studying airborne transmission in the built environment. In: Building Simulation. Springer, pp. 1–8.

Almstrand, A.-C., Bake, B., Ljungström, E., Larsson, P., Bredberg, A., Mirgorodskaya, E., Olin, A.-C., 2010. Effect of airway opening on production of exhaled particles. Journal of applied physiology 108 (3), 584–588.

Asadi, S., Cappa, C. D., Barreda, S., Wexler, A. S., Bouvier, N. M., Ristenpart, W. D., 2020. Efficacy of masks and face coverings in controlling outward aerosol particle emission from expiratory activities. Scientific reports 10 (1), 1–13.

Asadi, S., Wexler, A. S., Cappa, C. D., Barreda, S., Bouvier, N. M., Ristenpart, W. D., 2019. Aerosol emission and superemission during human speech increase with voice loudness. Scientific reports 9 (1), 1–10.

Bailey, E. F., Hoit, J. D., 2002. Speaking and breathing in high respiratory drive. Journal of Speech, Language, and Hearing Research.

Berlanga, F., Olmedo, I., Ruiz de Adana, M., 2017. Experimental analysis of the air velocity and contaminant dispersion of human exhalation flows. Indoor Air 27 (4), 803–815.

Buonanno, G., Morawska, L., Stabile, L., 2020a. Quantitative assessment of the risk of airborne transmission of sars-cov-2 infection: Prospective and retrospective applications. Environment International 145, 106112. URL https://www.sciencedirect.com/science/article/pii/S0160412020320675

Buonanno, G., Stabile, L., Morawska, L., 2020b. Estimation of airborne viral emission: quanta emission rate of sars-cov-2 for infection risk assessment. Environment International, 105794.

Cahours, X., Prasad, K., 2018. A review of electronic cigarette use behaviour studies. Beiträge zur Tabakforschung International/Contributions to Tobacco Research 28 (2), 81–92.

Dautzenberg, B., Bricard, D., 2015. Real-time characterization of e-cigarettes use: the 1 million puffs study. J. Addict. Res. Ther 6 (229.10), 4172.

Drewnick, F., Pikmann, J., Fachinger, F., Moormann, L., Sprang, F., Borrmann, S., 2021. Aerosol filtration efficiency of household materials for homemade face masks: Influence of material properties, particle size, particle electrical charge, face velocity, and leaks. Aerosol Science and Technology 55 (1), 63–79.

Farsalinos, K. E., Polosa, R., 2014. Safety evaluation and risk assessment of electronic cigarettes as tobacco cigarette substitutes: a systematic review. Therapeutic advances in drug safety 5 (2), 67–86.

Fears, A. C., Klimstra, W. B., Duprex, P., Hartman, A., Weaver, S. C., Plante, K., Mirchandani, D., Plante, J., Aguilar, P. V., Fernandez, D., et al., 2020. Comparative dynamic aerosol efficiencies of three emergent coronaviruses and the unusual persistence of sars-cov-2 in aerosol suspensions. medRxiv.

Floyd, E. L., Queimado, L., Wang, J., Regens, J. L., Johnson, D. L., 2018. Electronic cigarette power affects count concentration and particle size distribution of vaping aerosol. PloS one 13 (12), e0210147.

Gao, N., Niu, J., 2007. Modeling particle dispersion and deposition in indoor environments. Atmospheric environment 41 (18), 3862–3876.

Gao, N., Niu, J., Morawska, L., 2008. Distribution of respiratory droplets in enclosed environments under different air distribution methods. In: Building simulation. Vol. 1. Springer, pp. 326–335.

Ghaem-Maghami, E., 2006. The passive scalar concentration and velocity fields of isolated turbulent puffs.

Ghaem-Maghami, E., Johari, H., 2010. Velocity field of isolated turbulent puffs. Physics of Fluids 22 (11), 115105.

Gupta, J., Lin, C.-H., Chen, Q., 2009. Flow dynamics and characterization of a cough. Indoor air 19 (6), 517–525.

Gupta, J. K., Lin, C.-H., Chen, Q., 2010. Characterizing exhaled airflow from breathing and talking. Indoor air 20 (1), 31–39.

He, Q., Niu, J., Gao, N., Zhu, T., Wu, J., 2011. Cfd study of exhaled droplet transmission between occupants under different ventilation strategies in a typical office room. Building and Environment 46 (2), 397–408.

Hinds, W. C., 1999. Aerosol technology: properties, behavior, and measurement of airborne particles. John Wiley & Sons.

Hoshiko, M. S., 1965. Lung volume for initiation of phonation. Journal of applied physiology 20 (3), 480–482.

Hsiang, S., Allen, D., Annan-Phan, S., Bell, K., Bolliger, I., Chong, T., Druckenmiller, H., Huang, L. Y., Hultgren, A., Krasovich, E., et al., 2020. The effect of large-scale anti-contagion policies on the covid-19 pandemic. Nature 584 (7820), 262–267.

Ivanov, M., 2019. Exhaled air speed measurements of respiratory air flow, generated by ten different human subjects, under uncontrolled conditions. In: E3S Web of Conferences. Vol. 111. EDP Sciences.

Jayaweera, M., Perera, H., Gunawardana, B., Manatunge, J., 2020. Transmission of covid-19 virus by droplets and aerosols: A critical review on the unresolved dichotomy. Environmental Research, 109819.

Johnson, G., Morawska, L., Ristovski, Z., Hargreaves, M., Mengersen, K., Chao, C. Y. H., Wan, M., Li, Y., Xie, X., Katoshevski, D., et al., 2011. Modality of human expired aerosol size distributions. Journal of Aerosol Science 42 (12), 839–851.

Klompas, M., Baker, M. A., Rhee, C., 2020. Airborne transmission of sars-cov-2: theoretical considerations and available evidence. Jama.

Kulkarni P, B. P. A., K, W. (Eds.), 2011. Aerosol Measurement, Principles, Techniques, and Applications. John Wiley & Sons.

Lechasseur, A., Altmejd, S., Turgeon, N., Buonanno, G., Morawska, L., Brunet, D., Duchaine, C., Morissette, M. C., 2019. Variations in coil temperature/power and e-liquid constituents change size and lung deposition of particles emitted by an electronic cigarette. Physiological reports 7 (10), e14093.

Matthews, T., Thompson, C., Wilson, D., Hawthorne, A., Mage, D., 1989. Air velocities inside domestic environments: an important parameter in the study of indoor air quality and climate. Environment International 15 (1-6), 545–550.

McNeill, A., Brose, L. S., Calder, R., Bauld, L., Robson, D., 2018. Evidence review of e-cigarettes and heated tobacco products 2018. A report commissioned by Public Health England. London: Public Health England 6.

Morawska, L., Cao, J., 2020. Airborne transmission of sars-cov-2: The world should face the reality. Environment International, 105730.

Morawska, L., Johnson, G., Ristovski, Z., Hargreaves, M., Mengersen, K., Corbett, S., Chao, C. Y. H., Li, Y., Katoshevski, D., 2009. Size distribution and sites of origin of droplets expelled from the human respiratory tract during expiratory activities. Journal of Aerosol Science 40 (3), 256–269.

Morawska, L., Milton, D. K., 2020. It is time to address airborne transmission of coronavirus disease 2019 (covid-19). Clinical Infectious Diseases.
NASEM, 2018. Public health consequences of e-cigarettes: a consensus study report of the national academies of sciences, engineering, and medicine.
Nazaroff, W. W., 2004. Indoor particle dynamics. Indoor air 14 (Supplement 7), 175–183.
Nicas, M., Nazaroff, W. W., Hubbard, A., 2005. Toward understanding the risk of secondary airborne infection: emission of respirable pathogens. Journal of occupational and environmental hygiene 2 (3), 143–154.
Polosa, R., O'Leary, R., Tashkin, D., Emma, R., Caruso, M., 2019. The effect of e-cigarette aerosol emissions on respiratory health: a narrative review. Expert review of respiratory medicine 13 (9), 899–915.
RCP, 2016. Nicotine without smoke Tobacco harm reduction. Royal College of Physicians of London.
Ruzer, L. S., Harley, N. H., 2012. Aerosols handbook: measurement, dosimetry, and health effects. CRC press.
Shiu, E. Y., Leung, N. H., Cowling, B. J., 2019. Controversy around airborne versus droplet transmission of respiratory viruses: implication for infection prevention. Current opinion in infectious diseases 32 (4), 372–379.
Sickbert-Bennett, E. E., Samet, J. M., Clapp, P. W., Chen, H., Berntsen, J., Zeman, K. L., Tong, H., Weber, D. J., Bennett, W. D., 2020. Filtration efficiency of hospital face mask alternatives available for use during the covid-19 pandemic. JAMA Internal Medicine 180 (12), 1607–1612.
Sommerstein, R., Fux, C. A., Vuichard-Gysin, D., Abbas, M., Marschall, J., Balmelli, C., Troillet, N., Harbarth, S., Schlegel, M., Widmer, A., 2020. Risk of sars-cov-2 transmission by aerosols, the rational use of masks, and protection of healthcare workers from covid-19. Antimicrobial Resistance & Infection Control 9 (1), 1–8.
Stadnytskyi, V., Bax, C. E., Bax, A., Anfinrud, P., 2020. The airborne lifetime of small speech droplets and their potential importance in sars-cov-2 transmission. Proceedings of the National Academy of Sciences 117 (22), 11875–11877.
Sussman, R. A., Golberstein, E., Polosa, R., 2020. Aerial transmission of sars-cov-2 virus (and pathogens in general) through environmental e-cigarette aerosol. medRxiv.
Sussman, R. A., Golberstein, E., Polosa, R., 2021. Aerial transmission of the sars-cov-2 virus through environmental e-cigarette aerosols: implications for public policies. International Journal of Environmental Research and Public Health 18, 1437.
Tcharkhtchi, A., Abbasnezhad, N., Seydani, M. Z., Zirak, N., Farzaneh, S., Shirinbayan, M., 2020. An overview of filtration efficiency through the masks: Mechanisms of the aerosols penetration. Bioactive materials 6 (1), 106–122.
Ueki, H., Furusawa, Y., Iwatsuki-Horimoto, K., Imai, M., Kabata, H., Nishimura, H., Kawaoka, Y., 2020. Effectiveness of face masks in preventing airborne transmission of sars-cov-2. MSphere 5 (5).
Van Doremalen, N., Bushmaker, T., Morris, D. H., Holbrook, M. G., Gamble, A., Williamson, B. N., Tamin, A., Harcourt, J. L., Thornburg, N. J., Gerber, S. I., et al., 2020. Aerosol and surface stability of sars-cov-2 as compared with sars-cov-1. New England Journal of Medicine 382 (16), 1564–1567.
Vuorinen, V., Aarnio, M., Alava, M., Alopaeus, V., Atanasova, N., Auvinen, M., Balasubramanian, N., Bordbar, H., Erästö, P., Grande, R., et al., 2020. Modelling aerosol transport and virus exposure with numerical simulations in relation to sars-cov-2 transmission by inhalation indoors. Safety Science 130, 104866.
Wang, J., Chow, T.-T., 2011. Numerical investigation of influence of human walking on dispersion and deposition of expiratory droplets in airborne infection isolation room. Building and Environment 46 (10), 1993–2002.
Wei, J., Li, Y., 2015. Enhanced spread of expiratory droplets by turbulence in a cough jet. Building and Environment 93, 86–96.

Figures

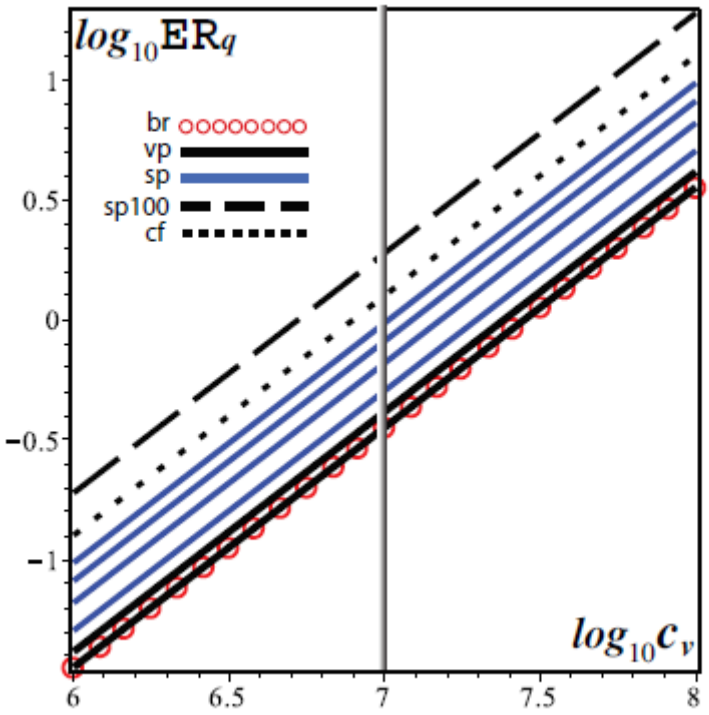

Figure 1

Quanta emission rates. The curves display ERq (quanta/hour) as a function of viral load cv (RNA copies/mL) for various expiratory activities: rest breathing (br), low and high intensity vaping (vp), speaking (bottom to top) 10; 20; 30; 40% of the hour (sp), coughing (cf) and speaking 100% of the time (sp100). Numerical values of ERq for cv = 107 RNA copies/mL (vertical line) are listed and discussed in the text. The ratios between these activities and rest breathing (taken as the case control scenario) is displayed in figure 4.

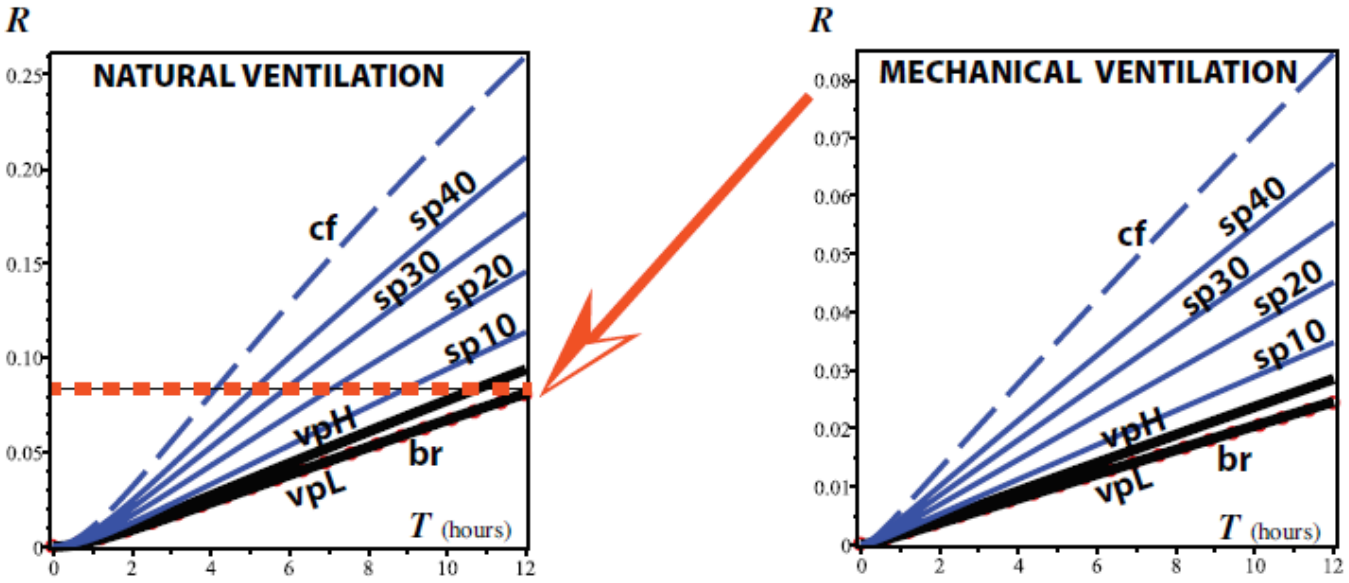

Figure 2

Infection risk in a home environment. The curves display R as a function of exposure time T from (6). The abbreviations br, vpL, vpH, sp10, sp20, sp30, sp40 and cf stand for rest breathing, vaping low intensity, vaping high intensity (upper end option), speaking for 10, 20, 30, 40,% of time and coughing. Notice the dramatic reduction of R achieved by mechanical ventilation (moderate air exchange rate of 3=h). Also: the curves for the risks from vaping (full range of intensities) are practically indistinguishable from that of the case control scenario of rest breathing (red circles).

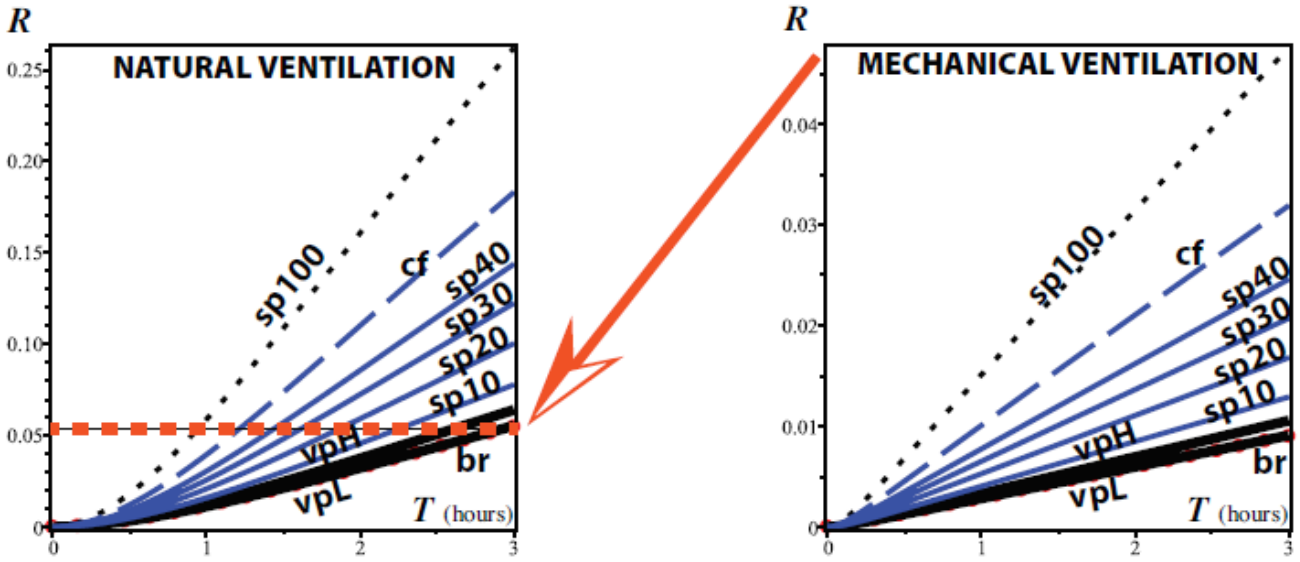

Figure 3

Infection risk in a restaurant. The same abbreviations as in figure 2 plus sp100 (speaking 100% of the time, a possible outcome when spending 3 hours in a restaurant). As in figure 2, mechanical ventilation (air exchange rate 9:6=h) achieves a dramatic reduction of R and the curves for the risks from vaping are practically indistinguishable from the curve of the control case scenario of rest breating (red circles).

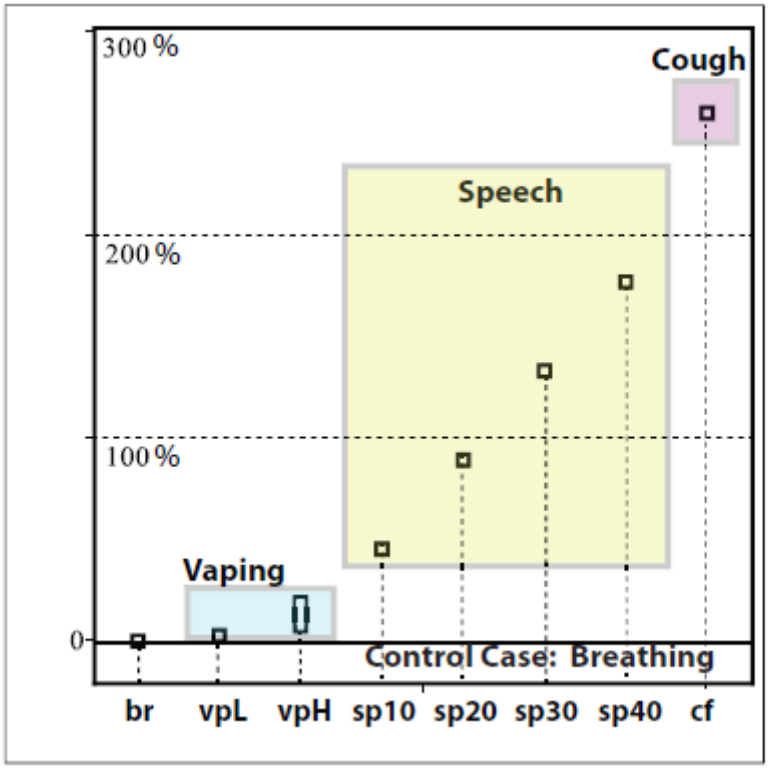

Figure 4

Added percentage risks of expiratory activities with respect to the control case scenario of rest breathing. The percentage values with respect to the control case are: low intensity vaping 1.3% (vpL), high intensity vaping 5.2- 17.7% (vpH), speaking 44% (sp10), 88% (sp20), 132% (sp30), 176% (sp40) for 10%, 20%, 30%, 40% of time, coughing 259% 30 times per hour (cf). These values were obtained from (ε - 1) x 100 for ε defined for these expiratory activities by (8)–(10).